Journal of Hydrology xxx (2011) xxx–xxx

Contents lists available at SciVerse ScienceDirect

Journal of Hydrology

journal homepage: www.elsevier.com/locate/jhydrol

Numerical modelling of spatio-temporal thermal heterogeneity in a complex river system

Jonathan L. Carrivick [a,*], Lee E. Brown [a], David M. Hannah [b], Andy G.D. Turner [a]

[a] School of Geography, University of Leeds, Leeds LS2 9JT, UK
[b] School of Geography, Earth and Environmental Science, University of Birmingham, Birmingham B15 2TT, UK

ARTICLE INFO

Article history:
Received 26 October 2011
Accepted 11 November 2011
Available online xxxx
This manuscript was handled by Konstantine P. Georgakakos, Editor-in-Chief, with the assistance of Vincent S. Neary, Associate Editor

Keywords:
Water temperature
Arctic
Heat budget
Heat transport
Glacier
Glacial river

SUMMARY

Accurate quantification and effective modelling of water temperature regimes is fundamental to underpin projections of future Arctic river temperature under scenarios of climate and hydrological change. We present results from a deterministic two-dimensional hydrodynamic model coupled with a heat transfer model that includes horizontal advection and vertical water surface energy fluxes. Firstly, we model longitudinal, lateral and temporal thermal heterogeneity of a braided reach of an Arctic river; Kårsajökk, Sweden. Model performance was assessed against water temperature data collected at 11 monitoring sites for two independent 1-week time periods. Overall, model performance was strongest (r values >0.9, *RMSEs* ~ 0.6 °C and *ME* < 0.4 °C) for main channel sites with relatively deep fast-flows where water temperature was comparatively low and stable. However, model performance was poorer for sites characterised by shallow and/or temporarily-stagnant streams at the lateral margins of the braidplain, where a lag of 60–90 min persisted between the modelled and measured water temperatures. Secondly, we present novel automated statistical analyses and quantify channel thermal connectivity and complexity. Our results lead us to suggest that with further development our modelling approach offers new opportunities for scenario-based predictions of response to environmental change and to assess anthropogenic impacts on water temperature.

1. Introduction

Water temperature is regarded widely as a 'master' water quality variable in aquatic systems due to its influence on a host of physical, chemical, and biological processes (Hawkins et al., 1997; Hannah et al., 2008). The study of thermal variability in rivers has a long history (Webb et al., 2008) but aquatic scientists still encounter problems in quantifying river thermal regime dynamics accurately. Current understanding of river temperature variability revolves largely around data collected from single sites. Whilst some researchers have adopted multi-site temperature recording campaigns to widen the scale of investigation (e.g. Arscott et al., 2001; Brown and Hannah, 2008), or distributed fibre-optic methods to increase temporal or spatial resolution (Selker et al., 2006), metre-scale lateral and longitudinal thermal dynamics remain very poorly constrained. Remote sensing approaches such as using thermal infra-red imagery have yielded some success in characterising the spatial heterogeneity of river thermal characteristics (Loheide and Gorelick, 2006; Tonolla et al., 2010) but suffer from limited temporal replication due to the expense of data acquisition and intensive image-processing (Cardenas et al., 2008).

Previous studies have shown the potential to numerically model river thermal dynamics from hydroclimatological, i.e. river discharge, water temperature and meteorological data collected at single sites (Sinokrot and Stefan, 1993; Caissie et al., 2005). Westhoff et al. (2007) modelled water temperatures distributed along a single-thread channel under steady flow conditions and Younus et al. (2000) modelled water temperature for a single-thread channel with unsteady flow. However, the introduction of low cost (miniature) digital water temperature dataloggers (Webb et al., 2008), the increase in usability of differential Global Positioning Systems (dGPS) to rapidly create Digital Elevation Models (DEMs), and the development of 'two-dimensional' or 'distributed' hydrodynamic models that are able to include water column temperature have yet to be exploited jointly for analysing and understanding the connectivity and spatio-temporal thermal heterogeneity of (complex) river systems. New technological solutions incorporating these elements offer the potential to provide combined high spatial (metre-scale) and temporal (sub-hourly) resolution thermal data to inform accurate environmental impact studies (Caissie et al., 2005), to provide the means to incorporate thermal heterogeneity into the planning stage of river remediation schemes (e.g. Young and Collier, 2009; Hester and Gooseff, 2010), and to predict river ecosystem responses to environmental change (Durance and Ormerod, 2007).

* Corresponding author. Tel.: +44 0113 343 3324; fax: +44 0113 343 3308.
E-mail address: j.l.carrivick@leeds.ac.uk (J.L. Carrivick).

0022-1694/$ - see front matter © 2011 Published by Elsevier B.V.
doi:10.1016/j.jhydrol.2011.11.026

High-latitude environments are considered to be at severe risk of major changes due to climate change (e.g. Schiermeier, 2006). General circulation models of the climate system suggest above global-average rates of future warming in the Arctic, which will affect glacier mass-balance and, in turn, proglacial river system hydrology (Milner et al., 2009). The structural and functional biological characteristics of glacier-fed river ecosystems are known to be strongly influenced by water temperature (Hannah et al., 2007; Brown et al., 2007) but there have been few studies of the thermal regime of Arctic river systems (Brown and Hannah, 2007; Lammers et al., 2007). Thus, accurate quantification of present-day thermal regimes, coupled with computationally efficient solutions for predicting future change, is fundamental to underpin efforts to understand the wider implication of Arctic climate change.

This paper reports a study of spatio-temporal water temperature dynamics undertaken in Arctic Sweden. This is the first application of a two-dimensional heat transport model for rivers and therefore this study aims to: (1) present the two-dimensional heat transport model; (2) assess the performance of this model in a variety of channel types and under a variety of weather conditions; (3) use this model as a tool to examine spatial and temporal patterns in water temperature heterogeneity, and (4) use this model to infer processes of heat advection and dispersion in rivers.

2. Study site and field methods

Field data were obtained for a ~6 km part of the Kårsajökk river, which is in upper Kårsavagge near Abisko in Arctic Sweden (Fig. 1A). Kårsajökk is sourced primarily from Kårsaglaciaren, which is a ~2 km^2 glacier. Kårsajökk runs through tundra above the tree line and therefore it is openly exposed to the atmosphere without trees or shading from other vegetation. Topographic shading is assumed to be uniform across the reach since the valley floor is of gentle and uniform slopes and the river is central to the valley floor rather than abutted to hillslopes (Fig. 2B). The uppermost reach, which we focus on in this study, comprises a distinct main channel, a complex of braided channels and a longitudinally extensive lateral margin channel (Fig. 1C). The main channel is typically 4 m wide and 0.4–0.8 m deep, the depth varying diurnally due to snow and ice melt. Braided channels and the lateral margin channel are generally narrower and shallower than this although highly variable in space and through time. Across this upper reach channel substrate and (unstable) banks comprise cobble and gravel-sized clasts. The mid-reach of this part of Kårsajökk is a single-thread channel that runs within a 3–6 m deep bedrock canyon between sites 'Main 2' and 'Main 7' (Fig. 1C). The lowermost (eastern) reach of this part of Kårsajökk; from site 'Main 7' eastwards, is a lake delta and the streams here have a silty-sand channel bed and grass-covered stable banks (Fig. 1C).

This study focused on two time periods (26th–31st July and 24th–29th August, 2008) for application of the coupled hydrodynamic and temperature model. These periods were selected to avoid the complication of advected water and heat input from precipitation as identified by Brown and Hannah (2007) and Chikita et al. (2010). To characterise atmospheric conditions, meteorological variables were monitored using an Automatic Weather Station (AWS), which was located ~0.2 km from the snout of Kårsaglaciären and thus at the most westerly part of the study braidplain (Fig. 1). Air temperature and relative humidity were monitored using a Campbell CS215 probe. Incoming short-wave radiation was measured with a Skye Instruments SP1110 pyranometer. Wind speed and direction was measured using a RM Young 03002-5 CSL probe and stored on a Campbell CR200 datalogger.

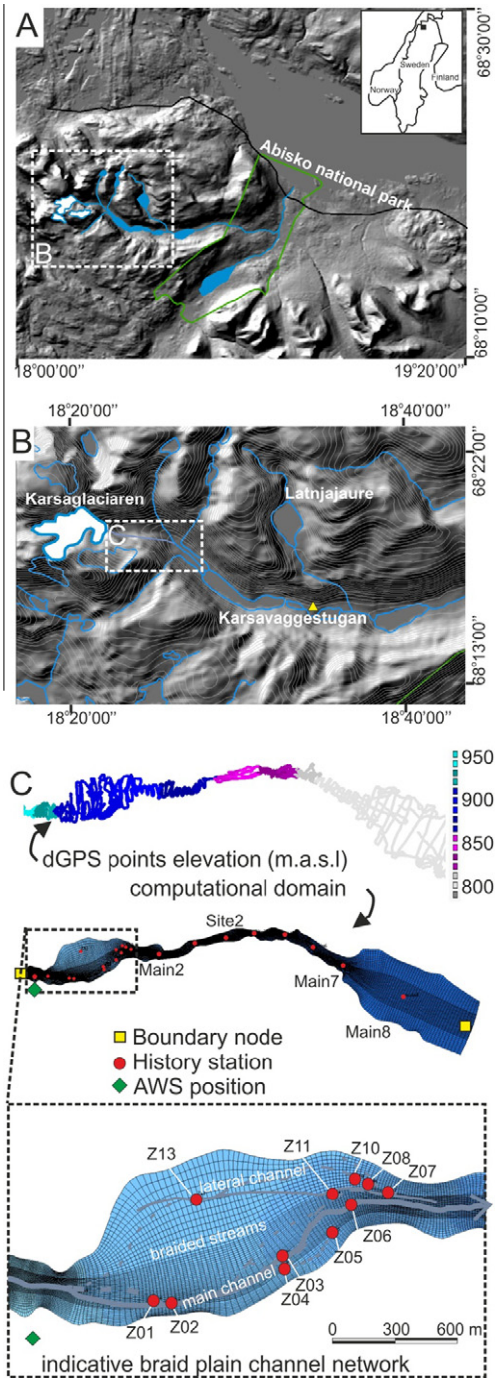

Fig. 1. The Kårsajokk River in Arctic Sweden (A) is predominantly fed from Kårsaglaciaren and comprises both single-thread and braided sections (B). High-resolution topography was gained via interpolation from an intensive dGPS RTK survey (C). This survey delimited the model domain, across which a computational mesh was constructed and refined to ~1 m horizontal resolution (C). Topography was mapped onto this mesh, and time-series data (Fig. 2) specified for the upstream and downstream boundary nodes. Modelled hydraulics and water temperature were computed in continuous space and at hourly time intervals and additionally at 11 sites Z01–Z13 where field measurements were made. Note that Z09 and Z12 do not exist.

River stage was measured at 0.1 km and 5.4 km from the Kårsaglaciaren snout using Druck PDCR1830 pressure transducers interfaced with Campbell Scientific CR10X dataloggers. The instantaneous slug salt-dilution method was used to estimate discharge for flows ranging from 0.3 to 0.9 m and a stage-discharge rating curve was constructed to yield discharge time-series. Water

Please cite this article in press as: Carrivick, J.L., et al. Numerical modelling of spatio-temporal thermal heterogeneity in a complex river system. J. Hydrol. (2011), doi:10.1016/j.jhydrol.2011.11.026

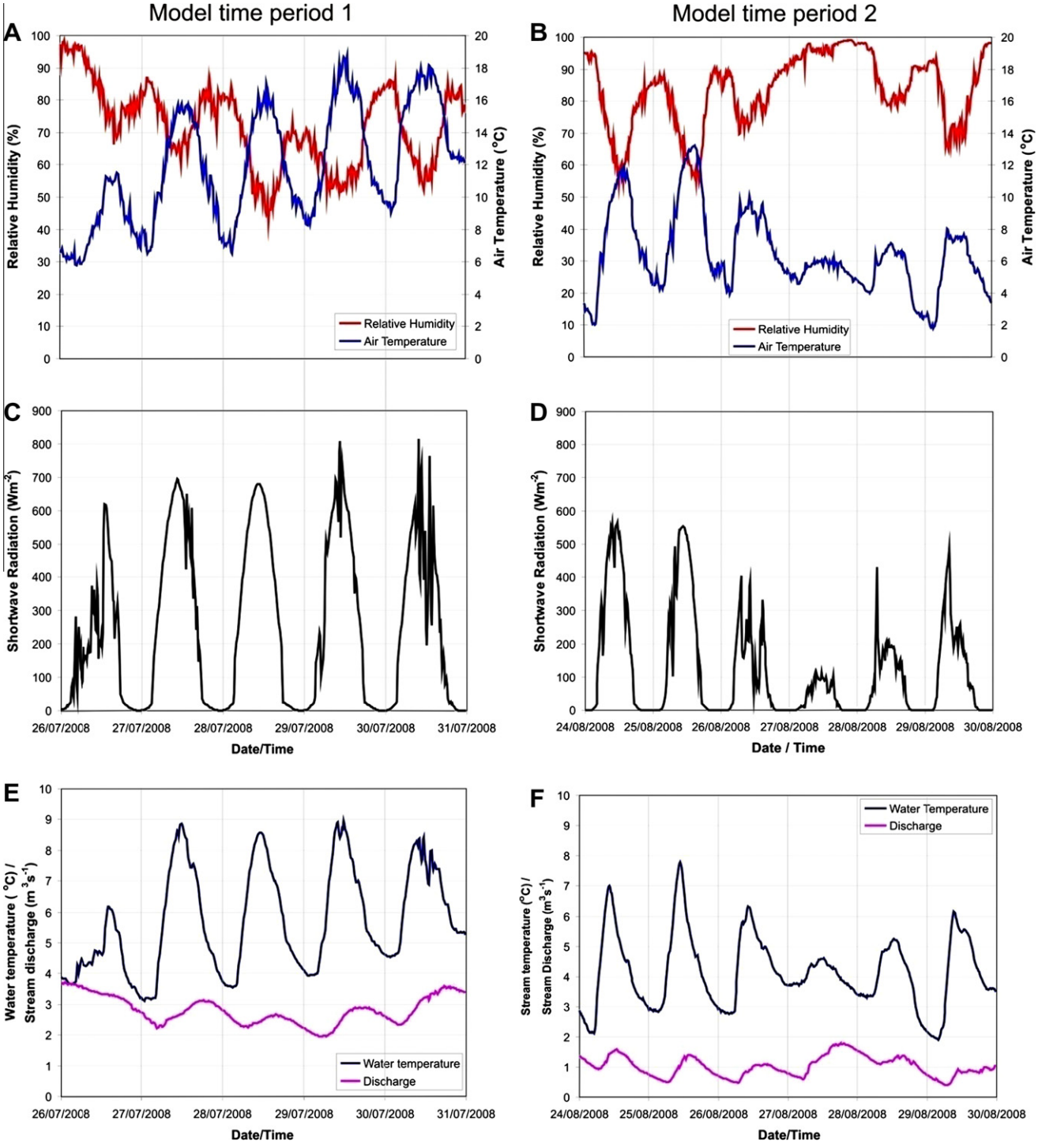

Fig. 2. Time-series data input to stream temperature model. Automatic Weather Station (AWS) records for air temperature and relative humidity (A, B) and incoming shortwave radiation (C, D) were specified uniformly across the entire model domain. In each time period the upstream boundary was specified for time-varying stream discharge and water temperature (E, F).

column temperature was monitored at 11 sites (Fig. 1C) along and across the braided river using Gemini Tinytag temperature dataloggers. At the river stage monitoring stations, water temperature was measured using Campbell Scientific CS547A temperature-electrical conductivity probes interfaced with Campbell CR10X dataloggers. All water temperature sensors were accurate to ±0.2 °C, cross-calibrated prior to field deployment, housed in radiation shields, logged values every 15 min and were continuously submerged. AWS and river stage sensors were scanned every 10 s and averages stored every 15 min. All datalogger clocks were synchronised.

3. Model domain specification

An intensive high-resolution differential Global Positioning System (dGPS) field survey run in Real Time Kinematic (RTK) mode at 1 s sampling interval enabled collection of a network of topographic points in three-dimensional space whilst walking

Please cite this article in press as: Carrivick, J.L., et al. Numerical modelling of spatio-temporal thermal heterogeneity in a complex river system. J. Hydrol. (2011), doi:10.1016/j.jhydrol.2011.11.026

across the study site (Fig. 1C). These points, which have typical point spacing of ~1 m, were then interpolated using an inverse distance weighting (IDW) algorithm to define a high-resolution (1 m grid cell size) Digital Elevation Models (DEMs). This DEM comprised the braided channel network and overbank topography and served to delineate lateral, longitudinal and vertical properties of the computational field for the hydrodynamic model. This computational field was created via user-specified splines that enabled automatic generation of a curvilinear grid (Fig. 1C). This grid was refined in the lateral and longitudinal directions to create a mesh at ~1 m resolution in horizontal space (Fig. 1C).

4. Hydrodynamic model

The hydrodynamic model used in this study is the open-source software Delft3D (WLDelft, 2011). Time-series of river discharge and water temperature (Fig. 2) were specified for upstream and downstream nodes (Fig. 1C). The model is forced to balance this upstream input and downstream output of water and thermal energy with additional exchange of thermal energy to/from the atmosphere. Several mesh nodes corresponding to field monitoring locations were ascribed as 'history stations' to extract modelled water temperature for assessment of model performance in space and time (Fig. 1C).

Delft3D solves the Navier–Stokes equations for an incompressible fluid: (1) under the shallow water assumption in which vertical momentum is reduced to a hydrostatic pressure, and (2) with the Boussinesq assumption that momentum transfer caused by turbulent eddies can be modelled with an 'eddy viscosity'. Governing laws of this model are described by the continuity and momentum equations, which are very well-known to be suitable for application to shallow river channels and braided river systems. They are fully documented within WLDelft (2011) and are not repeated here for brevity and because the focus of this paper is on the heat transport model. The model was run with a very short time step (0.001 min) and high spatial resolution; ~1 m mesh node spacing. We ran the hydrodynamic model with a single vertical layer; i.e. depth-averaged, and we considered that secondary circulation and sub-grid turbulence were negligible because of the high spatial resolution. Model bed elevation was fixed because field observations indicated that channel morphology remained unchanged during data collection. All model runs were primed with a 24-h simulation of base flow ($1\ m^3\ s^{-1}$) to 'pre-wet' the channel because this improved model performance of channel connectivity including hydraulic routing and diurnal expansion and contraction of the river channel network. Time integration of transport equations used an Alternating Direction Implicit (ADI) method, which is detailed in full by WLDelft (2011). However, due to the importance of the ADI for wetting and drying; i.e. for channel network expansion and contraction, such as that which occurs daily in proglacial braided river systems, we briefly summarise the method as follows. The first stage of the ADI method comprises the following four checks in the drying and flooding algorithm: (1) drying check for velocity points in the longitudinal direction, (2) drying check for velocity points in lateral direction and flooding check for velocity points in a lateral direction, (3) drying check for velocity points in a lateral direction during iterative solution for new water level, and (4) drying check (negative volumes) for water level points. In the second stage of the ADI method, directions are interchanged. Thus flow propagation, or 'wetting' was modelled as an advance of a kinematic wave over an initially dry bed and considered three factors: (1) bed elevation at a water level point (cell centre), (2) water level at velocity point, and (3) criteria for 'flooding'; i.e. setting a velocity and/or water level point to 'wet'. Overall, this method means that flow propagation could only proceed by one mesh cell per model time-step. Furthermore, whether a mesh cell is deemed to be wet or not is determined by a user-specified threshold of water depth, which was specified in this study as 0.1 m. For computational efficiency, meteorological and hydrological data were extracted at 2 h intervals; cf. 15 min resolution data acquisition in the field, for input to the hydrodynamic model.

5. Heat transport model

Water temperature was simulated using heat transport equations available within Delft3d. The simulations described herein consider heat as a conservative constituent. They consider vertical air–water interface energy exchanges and horizontal advective heat transfer due to fluid motion because these processes underpin hydraulics and thermal dynamics (Webb and Zhang, 1999; Hannah et al., 2004, 2008). The heat transport model was driven by our direct field measurements of air temperature, relative humidity and incoming short-wave radiation. These variables are all considered to be globally uniform across the entire model domain and thus shading and lapse-rates are not modelled. Energy balance terms not included are advective heat transport by precipitation and groundwater, and bed conduction and heat from fluid friction (cf. Hannah et al., 2004). Heat advection by groundwater (including hyporheic exchange) was not modelled because of: (1) the likely complex and high spatio-temporal variability of local groundsurface water interactions (e.g. Malcolm et al., 2005) that could not be accurately quantified across the relatively large study domain, and (2) uncertainties in estimating a reference temperature of groundwater. Bed heat flux was not modelled because it has been reported to be a small component of the overall river energy balance, particularly in summer (e.g. Webb and Zhang, 1997; Hannah et al., 2004, 2008). Bed friction is difficult to estimate accurately (Hannah et al., 2008) and indeed Moore et al. (2005) omit a bed friction term altogether.

The thermal capacity of a model grid cell depends on the water volume, with heat storage capacity increasing and thus sensitivity to the energy budget decreasing as the water volume increases (Sinokrot and Stefan, 1993). Heat transfer from the atmosphere is driven by the change in water surface '*S*' temperature T (K):

$$\frac{\partial T_s}{\partial t} = \frac{Q_N}{\rho_w c_p \Delta z_s} \tag{1}$$

where Q_N ($J\ m^{-2}\ s^{-1}$) is the total heat flux, c_p is the specific heat capacity of water ($4181\ J\ kg^{-1}\ K^{-1}$), ρ_w is the specific density of water ($1000\ kg\ m^{-3}$) and Δz_s (m) is the water depth. The total heat flux was specified as:

$$Q_N = Q_A + Q_K + Q_L + Q_E + Q_H \tag{2}$$

where Q_N = net heat exchange ($J\ m^{-2}\ s^{-1}$) as determined by both the horizontal advective heat flux Q_A ($J\ m^{-2}\ s^{-1}$) and the vertical water surface energy balance terms, namely the surface shortwave solar radiation flux Q_K ($J\ m^{-2}\ s^{-1}$), surface net longwave radiation flux Q_L ($J\ m^{-2}\ s^{-1}$), surface latent heat flux Q_E ($J\ m^{-2}\ s^{-1}$) and the surface sensible heat flux Q_H ($J\ m^{-2}\ s^{-1}$). Each of these heat flux components is detailed below.

Advective heat transfer in rivers occurs primarily due to fluid motion. Thus we model advective heat flux Q_A by simply regarding heat as a conservative constituent; i.e. a quantity that is held within a mesh cell and passed to adjacent mesh cells. Advection of heat is determined in the model by the horizontal (fluid) velocity in the Navier–Stokes equations where the deviatoric stress is calculated as the product of a tensor gradient of flow velocity and a viscosity (viscous stress) tensor (WLDelft, 2011). It is also

Please cite this article in press as: Carrivick, J.L., et al. Numerical modelling of spatio-temporal thermal heterogeneity in a complex river system. J. Hydrol. (2011), doi:10.1016/j.jhydrol.2011.11.026

assumed that the diffusion tensor is anisotropic for shallow water; i.e. the horizontal eddy diffusivity D_h ($m^2 s^{-1}$) far exceeds the vertical eddy diffusivity; $10 m^2 s^{-1}$. Horizontal velocity and thus the rate of heat advection was calculated using the ADI scheme as briefly outlined above in the 'hydrodynamic model' section and D_h is determined by:

$$D_h = \frac{u_c}{P} \tag{3}$$

where u_c is user-specified horizontal eddy viscosity ($0.01 m^2 s^{-1}$) and P is the dimensionless turbulence Prandtl–Schmidt number. The magnitude of u_c and thus of D_h is dependent on grid cell size because it is designed to average the deviatoric stress and thus to ignore small-scale vortices (or eddies) in fluid motion to simply calculate large-scale motion. We specified a single (constant) value for eddy viscosity (rather than computing an algebraic $k-L$ or $k-e$ turbulence model, where k is the turbulent kinetic energy, L is the mixing length and e is the dissipation rate of turbulent kinetic energy) for the whole model domain because the mesh cell size is near-uniform across the whole model domain and because flows are shallow and vertically well-mixed. Specification of u_c is thus essentially a consideration of turbulence, albeit within a model comprising depth-averaged flow. P approximates the ratio of momentum diffusivity (kinematic viscosity) and thermal diffusivity:

$$P = \frac{c_p \cdot \mu}{k} \tag{4}$$

where c_p = specific heat of water ($4181 J kg^{-1} K^{-1}$), μ = viscosity (Pa s), and k = thermal conductivity ($0.58 W m^{-2} K^{-1}$).

Shortwave (solar) radiation Q_K at the water surface is assumed to be partially absorbed on the surface S but ~50% can be transmitted into the water column (e.g. Hannah et al., 2004) as an exponential function of the water depth:

$$Q_K(z) = (1-\xi)Q_K \frac{e^{-\gamma z}}{1-e^{-\gamma H_{Turb}}} \tag{5}$$

where ξ (–) is the proportion of Q_K absorbed at the water surface, which is a function of the shortwave radiation wavelength. We use the default model value for ξ of 0.06 (and thus consider the shortwave radiation wavelength to be constant), although we note that previously 0.4 has been suggested (e.g. Edinger et al., 1968). We consider that the exact value of ξ does not matter too much because the water column mixes rapidly and the total heat flux by short-wave radiation is distributed within the water column. z is the water depth (m), and γ is the extinction coefficient (m^{-1}) related to the turbidity (H_{Turb}), which in the model is given by proxy as a Secchi depth (m):

$$\gamma = \frac{1.7}{H_{Turb}} \tag{6}$$

Net longwave radiation flux (Q_L) is the balance between incoming longwave radiation Q_{Lin} and emitted longwave radiation (Q_{Lout}). Q_{Lin} was estimated using the Stefan–Boltzmann Law:

$$Q_{Lin} = (1-r)\varepsilon\sigma T_a^4 \tag{7}$$

where $r = 0.03$ and is the fraction of Q_{Lin} that is reflected off the water surface according to Kirchoff's law (Oke, 1987; p. 12) and as given by $(1-\varepsilon)$ where ε is the emissivity of 0.97 for water (c.f. Oke, 1987). It is perhaps useful to note that remote sensing studies have suggested that sediment concentration has no effect on water emissivity (e.g. Liu et al., 1987). T_a (K) is the air temperature and σ (–) is the Stefan–Boltzmann constant of $5.67 \times 10^{-8} J s^{-1} m^{-2} K^{-4}$ (Oke, 1987).Q_{Lout} from the water column was given by the Stefan–Boltzmann Law (Oke, 1987):

$$Q_{Lout} = Q_{Lin}(1-\varepsilon) + \varepsilon\sigma T_s^4 \tag{8}$$

where σ (–) is the Stefan–Boltzmann constant of $5.67 \times 10^{-8} J s^{-1} m^{-2} K^{-4}$, T_s is the absolute water temperature (K), and where we assume a water emissivity ε of 0.97 as for Eq. (7).

Latent heat (Q_E) lost by evaporation or gained by condensation (E_V = evaporation/condensation rate, mm d^{-1}) was estimated by:

$$Q_E = L_V \rho_w E_V \tag{9}$$

where ρ_w is the specific weight of water ($1000 kg m^{-3}$) and L_V is the latent heat of vaporisation ($J kg^{-1}$):

$$L_V = 2.5 \times 10^6 - 2.3 \times 10^3 T_s \tag{10}$$

where T_s (K) is water temperature. The evaporation rate E_V defined as the volume of water evaporated per unit area per unit time is computed using Dalton's law of mass transfer:

$$E_V = fU_2(e_s - e_a) \tag{11}$$

where fU_2 is the Dalton number of 0.0012 multiplied by the average wind speed at 2 m above the surface and where the actual vapour pressure e_a (mbar) and the saturated vapour pressure e_s (mbar) were calculated by measurements of air temperature, relative humidity and water temperature, given that:

$$e_s = 23.38e^{18.1\frac{53303.3}{T_a}} \tag{12}$$

$$e_a = r_{hum} e_s \tag{13}$$

where T_a is the air temperature and r_{hum} = relative humidity, both of which are user-specified and time-varying.

Sensible heat transfer Q_H was estimated as the product of the Bowen ratio β (Bowen, 1926) and the latent heat flux Q_E:

$$Q_H = \beta Q_E \tag{14}$$

where the Bowen ratio:

$$\beta = \gamma \frac{(T_s - T_a)}{(e_w - e_a)} \tag{15}$$

where γ (–) is the psychrometric constant ($Pa K^{-1}$).

6. Model sensitivity

The sensitivity of modelled water temperature to selected parameters, excluding meteorological forcing, was assessed by a series of individual modelling experiments to isolate the influence of each parameter. For brevity, only results from one main channel site (Z07) and factors with high water temperature sensitivity are presented, namely turbidity (Fig. 3A), horizontal eddy diffusivity (Fig. 3B), and downstream boundary water temperature (Fig. 3C). Turbidity and downstream boundary water temperature displayed logarithmic relationships with the mean deviation of modelled water temperature from measured water temperature (Fig. 3D and F), whilst horizontal eddy diffusivity had an inverse linear relationship (Fig. 3E). However, turbidity had a negligible effect on modelled water temperature (Fig. 3A) because the majority of the model domain has shallow water depth. Water temperature at the downstream boundary node had the largest influence (Fig. 3C) and produces a forcing that propagated upstream as the model equilibrates. This forcing initially surprised us but we realise that in reality it is due to interactions of lake water with near-stagnant deltaic streams. In the model this forcing effect occurred between 'Main 7' and the downstream Boundary node (Fig. 1) and thus outside of our area of interest, which is on the uppermost (westernmost) reach; the braidplain.

Please cite this article in press as: Carrivick, J.L., et al. Numerical modelling of spatio-temporal thermal heterogeneity in a complex river system. J. Hydrol. (2011), doi:10.1016/j.jhydrol.2011.11.026

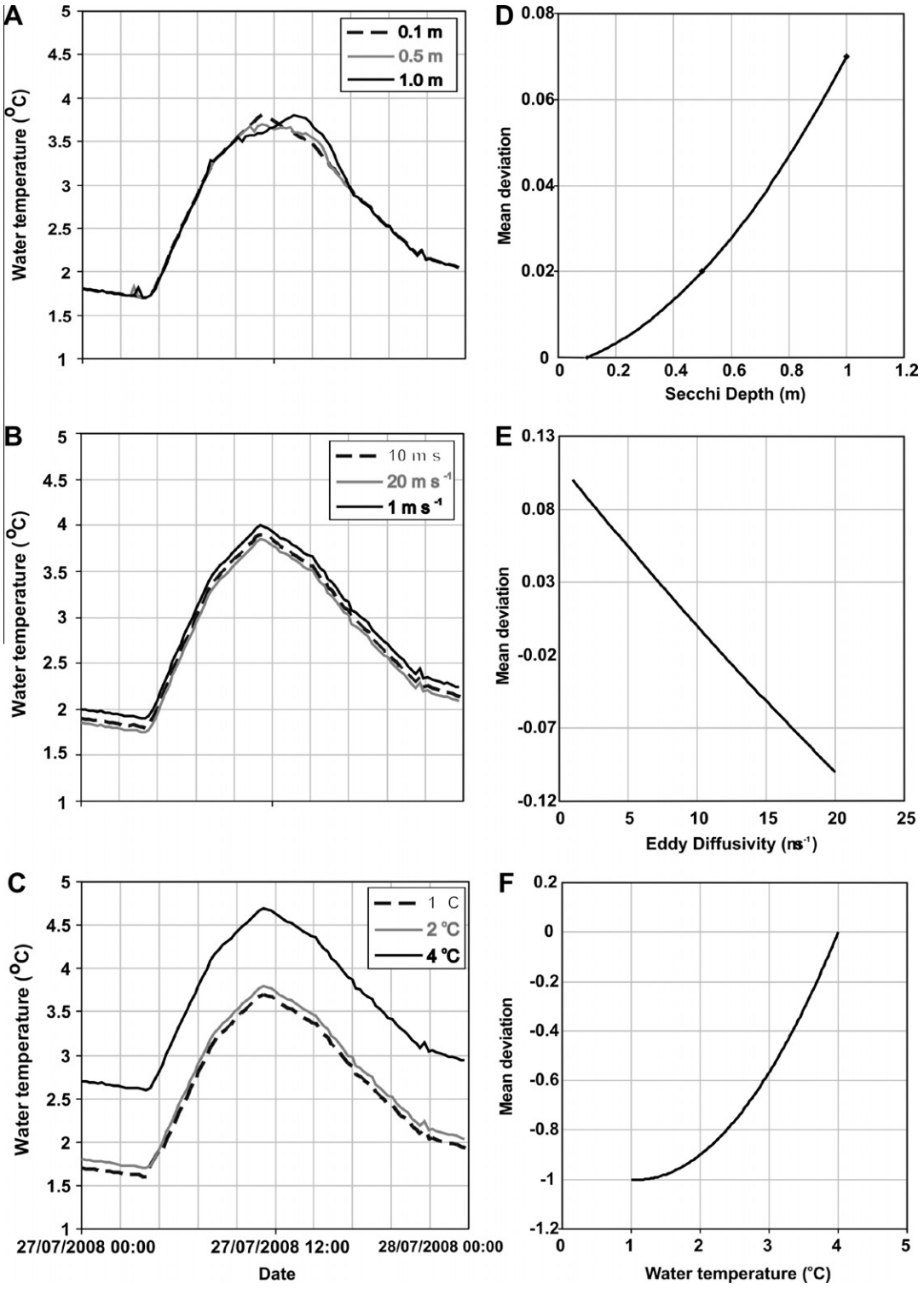

Fig. 3. Sensitivity analysis of water temperature to: Turbidity (expressed as 'Secchi depth' in Delft 3D) (A), eddy diffusivity (B), and downstream boundary water temperature (C). This control is characterised by an exponential relationship for turbidity (D), an inverse linear relationship for eddy diffusivity (E) and an exponential relationship for downstream boundary temperature (F).

7. Model performance

Model performance was evaluated quantitatively using a number of goodness of fit statistics (Table 1) as described and used by Hannah and Gurnell (2001) which assessed absolute numerical agreement, and similarity of form with time. Overall, model performance decreased as the range of water temperature at a site increased. During both time periods, it is clear that the model accurately replicated the shape, timing and magnitude of the diurnal river thermograph at a representative main channel site (Fig. 4A and D; Table 1). However, at sites in the centre of the braidplain in Period 1 the model tended to underestimate

Please cite this article in press as: Carrivick, J.L., et al. Numerical modelling of spatio-temporal thermal heterogeneity in a complex river system. J. Hydrol. (2011), doi:10.1016/j.jhydrol.2011.11.026

Table 1
Goodness of fit statistics to assess model performance for each time period, using >500 measured and modelled values. The mesh cell at point Z08 was not inundated in the model. All *r* values are statistically significant at a 95% confidence interval.

Site position	Site name	Max. obs-pred. (°C)	Min. obs-pred. (°C)	*ME* (°C)	*RMSE* (°C)	*r* (–)	Cross corr. mins. (*r*)
Model time Period 1: 26th–31st July, 2008							
Main channel	Z02	5.1	0	2.1	2.4	0.89	+15 (0.95)
	Z03	0.9	−0.6	0.1	0.3	0.97	+0 (0.97)
	Z04	1.3	−0.6	0.2	0.5	0.96	+0 (0.96)
	Z06	1.6	−0.6	0.4	0.6	0.96	+0 (0.96)
Mid-braidplain	Z05	5.7	−0.2	1.9	2.2	0.90	+45 (0.95)
	Z07	2.2	−0.2	1.0	1.1	0.95	+30 (0.96)
	Z11	4.1	−6.3	1.4	2.0	0.72	+45 (0.95)
Marginal channel	Z08	–	–	–	–	–	–
	Z10	5.1	−8.2	−0.5	3.4	0.71	+90 (0.85)
	Z13	13.8	−5.3	1.4	2.8	0.88	+75 (0.95)
Model time Period 2: 24th–30th August 2008							
Main channel	Z02	3.0	−1.2	0.8	1.2	0.83	+15 (0.89)
	Z03	2.7	−0.7	0.2	0.6	0.76	+15 (0.85)
	Z04	2.3	−1.6	−0.3	0.6	0.77	+15 (0.86)
	Z06	2.3	−1.6	−0.2	0.6	0.81	+0 (0.81)
Mid-braidplain	Z05	3.8	−2.3	0.9	1.5	0.79	+60 (0.90)
	Z07	2.4	−1.7	0.3	0.6	0.85	+60 (0.90)
	Z11	4.6	−12.2	−1.9	3.8	0.34	+90 (0.42)
Marginal channel	Z08	–	–	–	–	–	–
	Z10	10.8	−11.3	0.1	5.9	0.18	+30 (0.36)
	Z13	5.6	−10.5	0.3	4.2	0.74	+30 (0.76)

observations (Table 1), generated some unobserved oscillations, and lagged behind the timing of the daily peak water temperature by 1–1.5 h (Fig. 4B). This lag was most pronounced for sites at the lateral margins of the braidplain. Similarly, during Period 2 at this mid-braidplain site, the model did not accurately represent the timing of the daily peak water temperature (Table 1; Fig. 4E). At the marginal site, the modelled timing of peak water temperature was accurate, yet maximum and minimum water temperature was overestimated and underestimated (respectively) by ~3 °C in the first time period (Fig. 4C) and by >4 °C during the second time period (Fig. 3F).

8. Quantifying spatio-temporal variability in water temperature

A unified definition of spatial heterogeneity as a concept and as a definite formulation of its measurement have been lacking despite the importance of spatial heterogeneity in both theoretical and applied earth sciences (Li and Reynolds, 1994). This lack of definition has caused Li and Reynolds (1994) to question 'What is meant by the term "spatial heterogeneity?"' and 'How can it be measured?' The hydrodynamic model herein offered the opportunity to 'measure' spatio-temporal thermal heterogeneity by modelling water temperature across the entire wetted area of the model domain (Fig. 5). To take full advantage of this unprecedented spatio-temporal dataset a novel analysis of the temporal variability of water temperature across the entire model domain was achieved by exporting model grids at 1 h intervals to ASCII format and running a bespoke Java code (Turner, 2010) to interrogate these grids to produce a histogram, descriptive statistics and heterogeneity indices for each of these model grids. Thus a time-series of water temperature variability across the entire model domain was produced by this analysis of 1-h interval model grid outputs. Modelled water temperature had a histogram constructed from ~90,000 modelled (grid cell) values whilst the measured water temperature histogram comprised data from just 11 measured sites in the field. Thus, we calculated the hourly value of three higher-order spatial heterogeneity indices, namely dominance, diversity and evenness/equitability (e.g. Turner, 1990; Bower et al., 2004) to enable a comparison between modelled and measured water temperatures.

From spatially-gridded model output at hourly increments, we firstly computed the mean water temperature per mesh cell, which for the vast majority of the system was 0.5–2.0 °C (Fig. 5A). During Period 1, the minimum water temperature across the entire wetted area, which expanded and contracted diurnally in response to dynamic meltwater inputs from glacier- and snow-melt, was relatively uniform at 1–2 °C (Fig. 5B). There was shallow water (<0.1 m) and flow stagnation where the model simulated very high water temperature (Fig. 5B). The maximum water temperature was much more spatially variable compared to minimum water temperature, with main channel zones <4 °C and channels marginal to the braidplain reaching >12–14 °C (Table 1; Fig. 5C). Given this variability, we obtained the modelled range of water temperature as a proxy statistic for the water temperature regime (Fig. 5D).

The modelling in this project enables visualisation and quantitative analysis of the connectivity and thermal heterogeneity of the whole river system, in comparison to only relatively few single site water temperature measurements (Fig. 6). Specifically, the most salient feature is a clear diurnal cycle where water temperatures not only increase towards early afternoon but also become more 'diverse' in space (Fig. 6). While hourly mean values were not greatly different between the model and the field measurements for either time period, standard deviation was considerably different (Fig. 6A). Hourly modelled standard deviations were both of a greater magnitude and also had larger daily amplitude than standard deviations of hourly measured water temperatures (Fig. 6A).

The transient nature of thermal heterogeneity across the braidplain was further evident from grid-based analysis of modelled water temperatures. Measured and modelled skewness and kurtosis values calculated for hourly grids of water temperature were generally in disagreement with each other in direction, magnitude and temporal phase (Fig. 6B). This is a clear indication that dataloggers at 11 field measurement sites were not sufficient to fully capture the spatial or temporal variability of water temperatures. These indices of heterogeneity also showed diurnal cycles (Fig. 7) illustrating the increase and decrease of thermal heterogeneity

Please cite this article in press as: Carrivick, J.L., et al. Numerical modelling of spatio-temporal thermal heterogeneity in a complex river system. J. Hydrol. (2011), doi:10.1016/j.jhydrol.2011.11.026

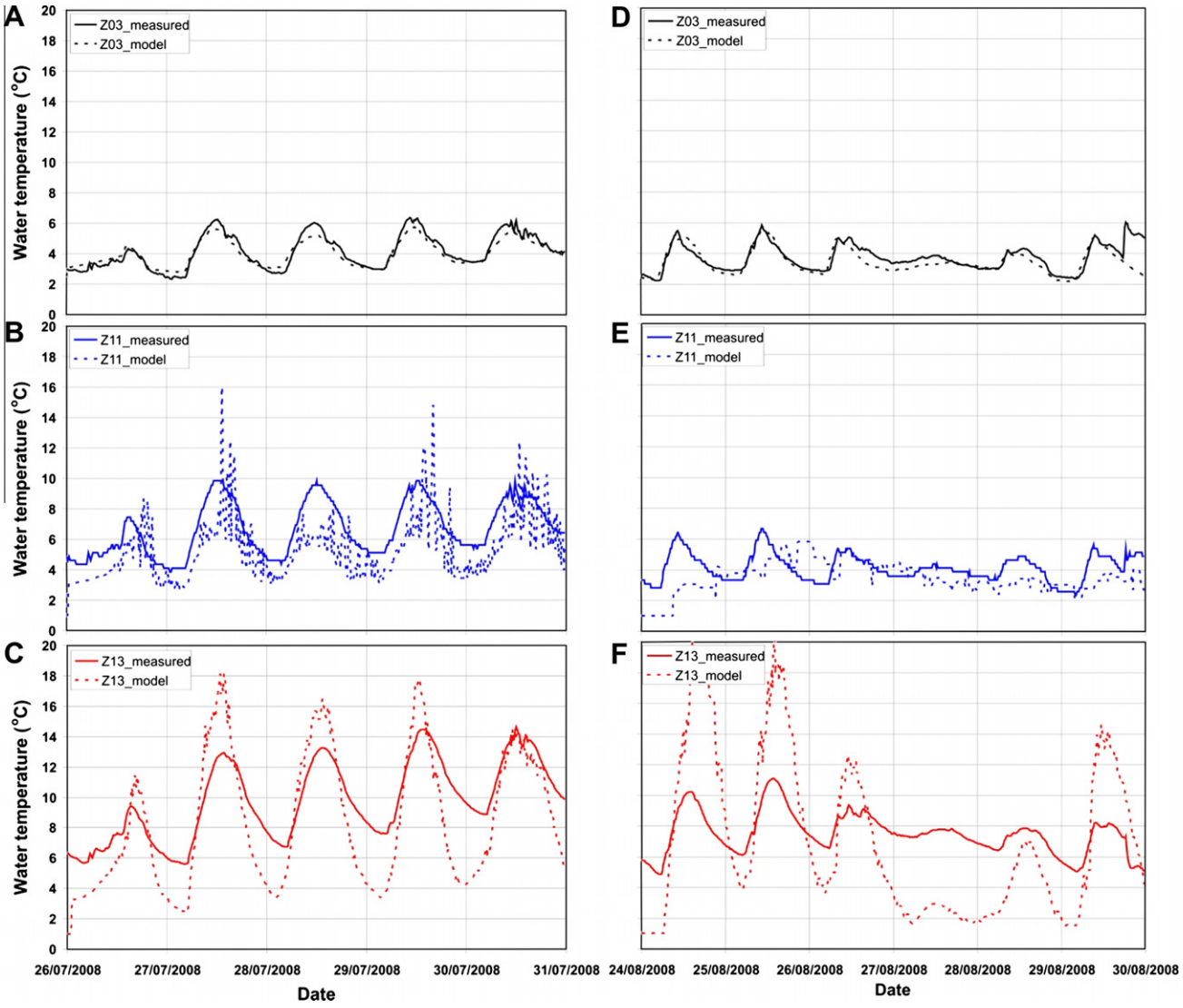

Fig. 4. Time series of monitored (solid lines) and modelled (dashed lines) water temperature for a main stream channel site (Z03), a site on braided channel (Z11), and a site on the lateral margins of the river network (Z13) for time period one 26–30 July 2008 (A, B, and C respectively), and for time period two 24–29 August, 2008 (D, E and F, respectively).

during the diurnal cycle. However, the diversity index was not as sensitive as the dominance index (Fig. 7), because it is calculated as the deviation from the maximum possible diversity at a given scale, i.e. in this case model cell size (Turner, 1990).

9. Discussion

This study has illustrated the potential utility of combining high-resolution digital elevation models, direct measurements of river water temperature at spatially discrete sites, meteorological observations and river hydrodynamic and heat transport models to understand spatio-temporal water column thermal heterogeneity. The thermal dynamics identified herein could not have been observed with air–water temperature regression or with stochastic methods (e.g. Caissie, 2006; Webb et al., 2008) because these common approaches are zero-dimensional and seek to simulate single-site measurements. Deterministic modelling has hitherto usually been carried out as a one-dimensional problem (Caissie, 2006) where temperature is simulated either along the principal longitudinal axis of a river, or at-a-point over a period of time (e.g. Chikita et al., 2010). This follows a commonly-held assertion that water temperature is relatively uniform with depth and that only small changes are observed in the lateral direction (i.e. that rivers are well-mixed cf. Clark et al., 1999). This may be the case for some hydraulically rough, single-thread stable channels for both steady flow conditions (e.g. Westhoff et al., 2007) and under unsteady flow conditions (e.g. Younus et al., 2000). However, our study illustrates that for a complex river system with unsteady flow conditions there are: (1) persistent thermal patterns between the main river channel and side channels, and (2) particularly strong lateral variability in water temperature.

The model described and applied herein generally simulated water temperature well in space and time when at-a-point predictions were extracted for comparison with the observed water temperature records. For example *RMSEs* for the main channel (0.3–2.4 °C) and for sites on the lateral margins of the river network (0.6–3.8 °C) are similar to the range of error obtained from other deterministic modelling studies that were focused relatively on single-site temporal changes or longitudinal changes (Marceau et al., 1986: 1.4–2.9 °C; Sinokrot and Stefan, 1993: <1.1 °C; Younus et al., 2000: 1.3 °C; Caissie et al., 1998: 0.6–1.7 °C; Caissie et al.,

Please cite this article in press as: Carrivick, J.L., et al. Numerical modelling of spatio-temporal thermal heterogeneity in a complex river system. J. Hydrol. (2011), doi:10.1016/j.jhydrol.2011.11.026

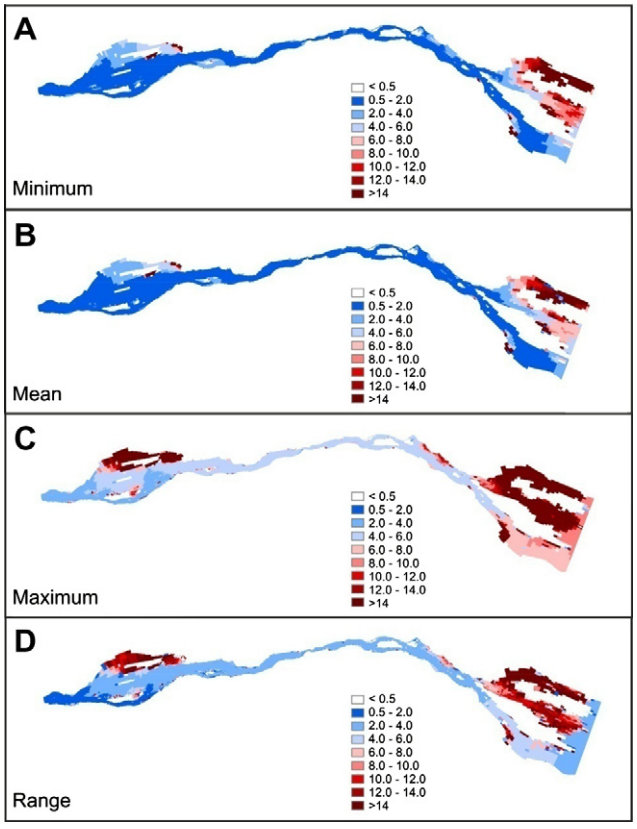

Fig. 5. Spatial distribution of modelled water temperature for time Period 1, illustrating the daily minimum (A), mean (B), maximum (C) and range (D) value for each mesh cell.

2005: 1.1–1.5 °C). With some knowledge of the field conditions, it can be stated that the variable 'range of water temperature' (Fig. 5D) discriminates clearly between water sources. Specifically, it is possible to identify (1) streams that are almost entirely glacier-fed (range 0.5–2.0 °C; Table 1; Fig. 5D), (2) streams that intermittently receive fluctuating water source contributions, and (3) streams at the lateral margin of the braidplain that are characterised by very high thermal heterogeneity (range >8 °C; Table 1; Fig. 5D).

The novel application of a heat transport model coupled to a hydrodynamic model, albeit with its inherent limitations, serves as a tool to infer dominant controls on water temperature in space and through time. The model performance in the main channel suggests that bed conduction heat fluxes; i.e. frictional, groundwater and hyporheic heat sources or sinks, are negligible for stable channels with persistent longitudinal connectivity. This negligible influence of bed heat flux for stable river channels is in agreement with the findings of Webb and Zhang (1997) and Hannah et al. (2004, 2008) for a temperate environment and alpine environments, respectively, but in disagreement with the suggestions of Story et al. (2003) and Cozzetto et al. (2006), which are studies in a temperate and polar environment, respectively. Modelled thermal oscillations for sites in the centre of the braidplain were not measured in the field and could be due to: (1) a modelled change in water source contributions and water (initial) temperature (cf. Cadbury et al., 2008) as the main channel over-spilled into the centre of the braidplain at high discharge, for example, (2) insufficient 'buffering' in the model of the instantaneous radiative flux, or (3) a lack of a land-surface heat model from non-wetted grid cells where specifically there could be an antecedent control of the temperature of the gravel bars prior to becoming inundated during episodes of flow network expansion (c.f. Burkholder et al., 2008; Cardenas, 2010). Additionally, we suggest that some high-frequency variability was not dampened because of a small thermal capacity limit (i.e. mesh cells size) and due to shallow water depths.

In explanation of the relatively poor performance of the model for marginal channel sites it is important to note that marginal channels are ephemeral as controlled by channel network changes; i.e. diurnal braidplain expansions and contractions. Our modelling of this ephemeral character may need to be modified for several reasons. Firstly, the hydraulic treatment of mesh cell wetting and drying assumes that a mesh cell is dry if zero velocity persists with a (user-specified) minimum water depth of 0.1 m. Although we only measured water temperature and not flow hydraulics at braidplain sites (Z01–Z13) we are confident in the wetting and drying (ADI) routine because the model has been tested against field data from a dam break outburst flood (Carrivick, 2007; Carrivick et al., 2009, 2010), which is an extreme case of a flow front propagating over a dry unconsolidated gravel bed. Secondly, the model specifies meteorological conditions 'globally' (i.e. uniformly over the whole model domain), which could be erroneous because lapse rates in temperature and moisture, and thus changes in atmospheric absorbance of radiation are not accounted for. Thirdly, our relatively poor modelling results from areas of marginal ephemeral channels hints that ground heat flux can be an important driver of water temperature; because ground heat flux is absent from the model, where water is shallow and slow-moving or stagnant, where exchange of heat from groundwater and hyporheic sources is pronounced (Hannah et al., 2009) or where hillslope processes are prevalent (e.g. Loheide and Gorelick, 2006).

There is some evidence that the performance of the model also depends on prevailing weather conditions. Model simulations of water temperature were less robust for Period 2. This period was characterised by a lower net radiative flux than Period 1 (Fig. 2D) when there was far more cloud cover. The inference is that radiation is the dominant heat transfer process and that the other heat fluxes were not so well modelled. There is clearly a need for future comparison of energy budget schemes to determine the relative importance (and model performance) of heat flux components. Additionally, we purposefully chose not to model days with rainfall because these heat transfers have to be explicitly measured and quantified before being written into a numerical model. We only possess summer field data on water temperatures. Therefore, further research is required to assess model performance across other temperature ranges or extremes and seasons.

Our modelling shows that spatio-temporal calculations of water temperature are crucial to consider the interaction of three key parts of deterministic models, particularly in systems with ephemeral and multi-scale components. These three parts are process-representations determined per mesh cell herein and include: (1) heat energy imported and exported, (2) thermal capacity exposed to that energy, and (3) antecedent water temperature raised/lowered by that heat exchange. The issues encountered in this study with modelling these three sets of processes are most evident in our sensitivity analyses, which show the dominance of the advective processes over dispersion in relatively shallow and fast-moving water, and in the fact that marginal channels are relatively poorly simulated. Channels at the lateral margin of the braidplain have very high width–depth ratios, a very small volume and consequently a large modelled thermal range. In addition, it is probable that marginal sites receive hydrological inputs from hillslopes and springs that will advect more thermally stable waters (Brown and Hannah, 2007); these hydrological fluxes are beyond representation in the current modelling scheme. Further investigation is required to determine if this reduced predictability is indicative of issues with either the water volume; i.e. thermal capacity, flow rate, hydraulic retention and time for equili-

Please cite this article in press as: Carrivick, J.L., et al. Numerical modelling of spatio-temporal thermal heterogeneity in a complex river system. J. Hydrol. (2011), doi:10.1016/j.jhydrol.2011.11.026

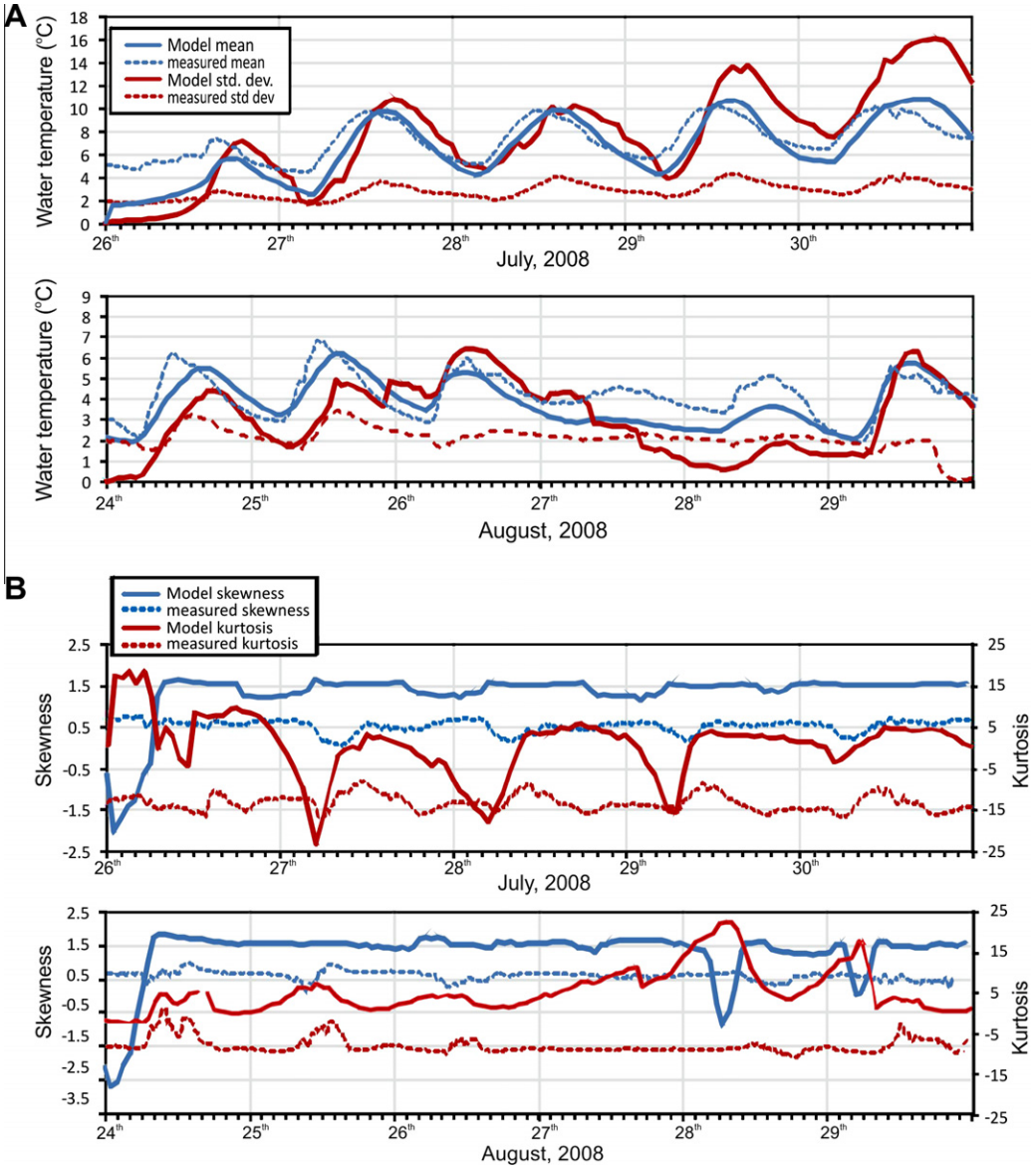

Fig. 6. Temporal distribution of modelled and measured water temperature heterogeneity for both time periods, illustrating the hourly mean and standard deviation (A), and the hourly skewness and kurtosis (B). The model results are of all wetted mesh cells; i.e. for the whole model domain.

bration. Alternatively, there may be a limit to the advection–dispersion performance linked to the size of the computational mesh because some river channels are narrower/shallower than the mesh resolution. This highlights the importance of accurate and high-resolution DEMs of channel bathymetry and overbank topography as well as (computationally efficient) high-resolution model meshes.

This study indicates the potential for deterministic models to represent thermal connectivity and spatio-temporal thermal heterogeneity in rivers with multiple channels and/or with significant lateral variability. A major benefit of deterministic models of water temperature is the potential to develop insights into spatio-temporal thermal heterogeneity, something that is not possible from sparse at-a-point field measurements. Thus, in contrast to previous studies focussing on the thermal 'heterogeneity' of river systems (e.g. Arscott et al., 2001; Brown and Hannah, 2008; Tonolla et al., 2010) we were able for the first time to highlight and quantify the coherence/complexity and robustness/sensitivity of patch-scale river water temperature distribution with both magnitude and temporal fluctuations. This emphasises that quantification of thermal heterogeneity is not straightforward and depends both on the scale and on the statistical approach adopted. For example, whilst the diversity, dominance and evenness indices all followed a clear and relatively smooth diurnal cycle (Fig. 7), evenness was notably more variable. This is because the evenness index responds to the probability that a pixel belongs to a patch type, and to the number of patch types and their proportions in a landscape. In this case, a patch is a group of grid cells with water temperature belonging to a 0.25 °C interval of the histogram. Evenness is thus a surrogate for not only the magnitude of spatial heterogeneity but it also appears to indicate the rate of change of that heterogeneity. Overall, with development this approach could be used to identify thermal pulses linked to the wetting and drying, and thus heating and cooling, of parts of the river system as individual channels activate and stagnate with avulsions and river network changes. For example, a very recent approach to couple models of surface and groundwater–hyporheic flows that focussed on biochemistry by Koch et al. (2011) could perhaps be extended to thermal dynamics. However, on the basis of the investigations in this study, we consider that should such significant channel avul-

Please cite this article in press as: Carrivick, J.L., et al. Numerical modelling of spatio-temporal thermal heterogeneity in a complex river system. J. Hydrol. (2011), doi:10.1016/j.jhydrol.2011.11.026

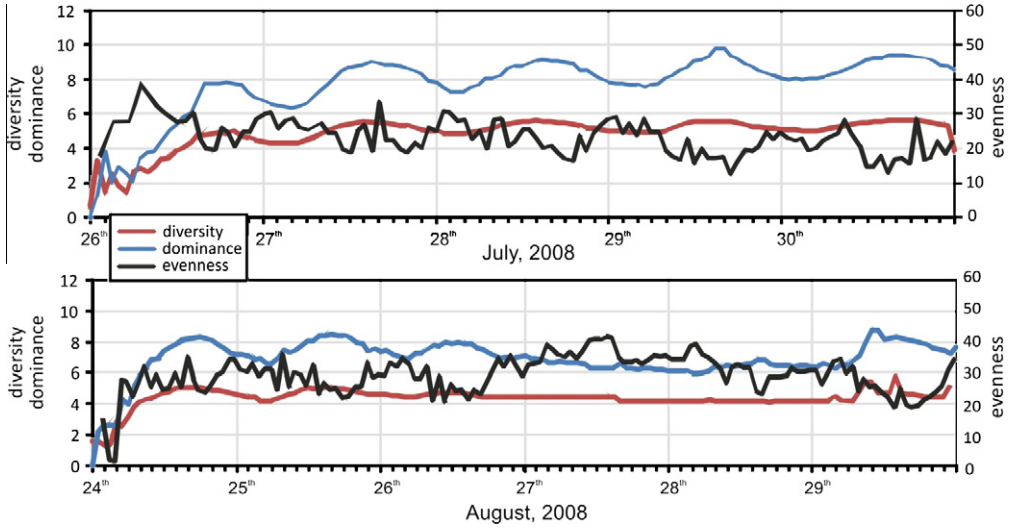

Fig. 7. Spatial heterogeneity indices calculated per hour for modelled water temperature model representations for all wetted mesh cells; i.e. across the whole model domain.

sions or network changes occur, for instance river expansion laterally overbank or across valley floors, knowledge of the antecedent ground temperature and thermal characteristics of the ground would be important for determining water temperature. Thus a land cover model and a land surface heat budget model would be required, as well as a hydrodynamic-heat transport model.

More widely, it is clear that further development of deterministic models could be especially suitable for applications such as analysing sensitivity to environmental change through scenario-based manipulations (Caissie et al., 2005). In the case of the Arctic, hydrological change will be dependent on a changing climate (Lammers et al., 2007) and as our modelling suggests most notably by changes in the radiation balance. Models should thus examine the effect of river discharge magnitude and timing and changing surface energy balance on water temperature. Other reach-based studies that would benefit from scenario-based two-dimensional modelling include those producing management plans to examine the interplay between climate, hydrology and geomorphology in situations where rivers are affected by riparian modification; for example Mitchell (1999) applied a regression model to the problem and Sridhar et al. (2004) applied a physically-based model, or those studies quantifying river rehabilitation or restoration works (e.g. Horne et al., 2004; Null et al., 2009). In such circumstances, a spatio-temporal representation of the river thermal regime would enable testing of various scenarios to find solutions to produce thermal heterogeneity commensurate with any ecological aims of a given restoration scheme.

10. Conclusions

This study presents governing equations and a method for coupling a heat transport model to a two-dimensional hydrodynamics model. It tests this method with application to a complex river system and evaluates this approach in comparison to at-a-point field measurements of high temporal resolution water temperature. We demonstrate for the first time how water temperature can be numerically modelled through time over two-dimensional space and analysed to discriminate thermal regimes dependent on longitudinal and lateral river hydrodynamics. This modelling has been achieved by exploiting the benefits of recent technological advances in digital surveying, automatic environmental sensors and hydrodynamic modelling.

To evaluate this novel modelling approach, we examined model goodness of fit statistics that yield r values >0.9, $RMSEs \sim 0.6$ °C and $ME < 0.4$ °C for main channels. However, model performance decreased for sites characterised by shallow and/or temporarily-stagnant water at the lateral margins of the braidplain. A lag of 60–90 min persisted between the modelled and measured water temperature for sites on the lateral margin of the braidplain. As a method for interpolating between multi-site observations, the model reveals flow pulses linked to the wetting and drying of the system as individual channels activate and stagnate with avulsions and river network changes, and shows how these are superimposed upon the diurnal thermal cycle. Future numerical modelling efforts should aim to develop the sensitivity analyses of this study into a full discrimination of the contributions of major heat flux components. In this manner, an understanding of fundamental energy transfer processes will aid model transferability to wider applications. Spatially-varied meteorological conditions should be considered to accommodate shading and sites with local microclimates due to topographic or riparian shading, for example. Future modelling will benefit from utilising not only field-deployed array of sensors, as in this study, but also infra-red cameras (Torgersen et al., 2001; Tonolla et al., 2010) that can yield calibration and validation data with spatial and temporal coverage akin to that of the model domain. Such scenario-based modelling and future projection of hydrological patterns and hydraulic conditions would also be of value in other studies, such as finding optimal solutions for river remediation (e.g. Hester and Gooseff, 2010) where changes in channel morphology or flow are likely to drive alterations to the thermal regime, or within studies concerned with heated effluent discharges.

Acknowledgements

JLC, LEB and DMH were in receipt of Transnational Access Programme (ATANS) FP6 506004 grants awarded through the Abisko Scientific Research Station. JLC and LEB were also supported by the Royal Geographical Society H.R. Mill Trust Fund (GFG 08/07) and by a School of Geography (Leeds) research development fund grant. Katherine Arrell, David Ashley, Christopher Mellor, Alexander Milner and Clare Plant provided much appreciated assistance in the field.

References

Arscott, D.B., Tockner, K., Ward, J.V., 2001. Thermal heterogeneity along a braided floodplain river (Tagliamento River, northeastern Italy). Can. J. Fish. Aquat. Sci. 58, 2359–2373.

Bowen, I.S., 1926. The ratio of heat losses by conduction and evaporation from any water surface. Phys. Rev. 27, 779–787.
Bower, D., Hannah, D.M., McGregor, G.R., 2004. Techniques for assessing the climatic sensitivity of river flow regimes. Hydrol. Process. 18, 2515–2543.
Brown, L.E., Hannah, D.M., 2007. Alpine stream temperature response to storm events. J. Hydrometeorol. 8, 952–967.
Brown, L.E., Hannah, D.M., 2008. Spatial heterogeneity of water temperature across an alpine river basin. Hydrol. Process. 22, 954–967.
Brown, L.E., Hannah, D.M., Milner, A.M., 2007. Vulnerability of alpine stream biodiversity to shrinking glaciers and snowpacks. Glob. Change Biol. 13, 958–966.
Burkholder, B.K., Grant, G.E., Haggerty, R., Khangaonkar, T., Wampler, P.J., 2008. Influence of hyporheic flow and geomorphology on temperature of a large, gravel-bed river, Clackamas River, Oregon, USA. Hydrol. Process. 22, 941–953.
Cadbury, S.L., Hannah, D.M., Milner, A.M., Pearson, C.P., Brown, L.E., 2008. Stream temperature dynamics within a New Zealand glacierized river basin. River Res. Appl. 24, 68–89.
Caissie, D., 2006. The thermal regime of rivers: a review. Freshw. Biol. 51, 1389–1406.
Caissie, D., El-Jabi, N., St-Hilaire, A., 1998. Stochastic modelling of water temperatures in a small stream using air to water relations. Can. J. Civ. Eng. 25, 250–260.
Caissie, D., Satish, M.G., El-Jabi, N., 2005. Predicting river water temperatures using the equilibrium temperature concept with application on Miramichi River catchments (New Brunswick, Canada). Hydrol. Process. 19, 2137–2159.
Cardenas, M.B., 2010. Lessons from and assessment of Boussinesq aquifer modeling of a large fluvial island in a dam-regulated river. Adv. Water Resour. 33, 1359–1366.
Cardenas, M.B., Harvey, J.W., Packman, A.I., Scott, D.T., 2008. Ground-based thermography of fluvial systems at low and high discharge reveals complex thermal heterogeneity driven by flow variation and bioroughness. Hydrol. Process. 22, 980–986.
Carrivick, J.L., 2007. Modelling coupled hydraulics and sediment transport of a high-magnitude flood and associated landscape change. Ann. Glaciol. 45, 143–154.
Carrivick, J.L., Manville, V., Cronin, S., 2009. Modelling the March 2007 lahar from Mt Ruapehu. Bull. Volcanol. 71 (2), 153–169.
Carrivick, J.L., Manville, V., Graettinger, A., Cronin, S., 2010. Coupled fluid dynamics-sediment transport modelling of a Crater Lake break-out lahar: Mt. Ruapehu, New Zealand. J. Hydrol. 388, 399–413.
Chikita, K.A., Kaminaga, R., Kudo, I., Tomoyuki, W., Yongwon, K., 2010. Parameters determining water temperature of a proglacial stream: the Phelan creek and the Gulkana glacier, Alaska. River Res. Appl. 26, 995–1004.
Clark, E., Webb, B.W., Ladle, M., 1999. Microthermal gradients and ecological implications in Dorset rivers. Hydrol. Process. 13, 423–438.
Cozzetto, K., McKnight, D., Nylen, T., Fountain, A., 2006. Experimental investigations into processes controlling stream and hyporheic temperatures, Fryxell Basin, Antarctica. Adv. Water Resour. 29, 130–153.
Durance, I., Ormerod, S.J., 2007. Climate change effects on upland stream macroinvertebrates over a 25-year period. Glob. Change Biol. 13, 942–957.
Edinger, J.E., Duttweiler, D.W., Brady, R., 1968. The response of water temperature to meteorological conditions. Water Resour. Res. 4, 1137–1145.
Hannah, D.M., Gurnell, A.M., 2001. A conceptual, linear reservoir runoff model to investigate melt season changes in cirque glacier hydrology. J. Hydrol. 246, 123–141.
Hannah, D.M., Malcolm, I.A., Soulsby, C., Youngson, A.F., 2004. Heat exchanges and temperatures within a salmon spawning stream in the Cairngorms, Scotland: seasonal and sub-seasonal dynamics. Rivers Res. Apps. 20, 635–652.
Hannah, D.M., Brown, L.E., Milner, A.M., Gurnell, A.M., McGregor, G.R., Petts, G.E., Smith, B.P.G., Snook, D.L., 2007. Integrating climate-hydrology–ecology for alpine river systems. Aquat. Conserv.: Mar. Freshw. Ecosyst. 17, 636–656.
Hannah, D.M., Malcolm, I.A., Soulsby, C., Youngson, A.F., 2008. A comparison of forest and moorland stream microclimate, heat exchanges and thermal dynamics. Hydrol. Process. 22, 919–940.
Hannah, D.M., Malcolm, I.A., Bradley, C., 2009. Seasonal hyporheic temperature dynamics over riffle bedforms. Hydrol. Process. 23, 2178–2194.
Hawkins, C.P., Hogue, J.N., Decker, L.M., Feminella, J.W., 1997. Channel morphology, water temperature, and assemblage structure of stream insects. J. North Am. Benthol. Soc. 16, 728–749.
Hester, E.T., Gooseff, M.N., 2010. Moving beyond the banks: hyporheic restoration is fundamental to restoring ecological services and functions of streams. Environ. Sci. Technol. 44 (5), 1521–1525.
Horne, B.D., Rutherford, E.S., Wehrly, K.E., 2004. Simulating effects of hydro-dam alteration on thermal regime and wild steelhead recruitment in a stable-flow Lake Michigan tributary. Rivers Res. Apps. 20, 185–203.
Koch, J.C., McKnight, D.M., Neupauer, R.M., 2011. Simulating unsteady flow, anabranching, and hyporheic dynamics in a glacial meltwater stream using a coupled surface water routing and groundwater flow model. Water Resour. Res. 47, W05530.
Lammers, R.B., Pundsack, J.W., Shiklomanov, A.I., 2007. Variability in river temperature, discharge, and energy flux from the Russian pan-Arctic landmass. J. Geophys. Res. – Biogeosci. 112 (G4), G04S59.
Li, H., Reynolds, J.F., 1994. A simulation experiment to quantify spatial heterogeneity in categorical maps. Ecology 75, 2446–2455.
Liu, W.-Y., Field, R.T., Gantt, R.G., Klemas, V., 1987. Measurement of the surface emissivity of turbid waters. Remote Sens. Environ. 21, 97–109.
Loheide, S.P., Gorelick, S.M., 2006. Quantifying stream–aquifer interactions through the analysis of remotely sensed thermographic profiles and in situ temperature histories. Environ. Sci. Technol. 40, 3336–3341.
Malcolm, I.A., Soulsby, C., Youngson, A.F., Hannah, D.M., 2005. Catchment scale controls on groundwater—surface water interactions in the hyporheic zone: implications for salmon embryo survival. Rivers Res. Appl. 21, 977–989.
Marceau, P., Cluis, D., Morin, G., 1986. Comparaison des performances relatives à un modèle déterministe et à un modèle stochastique de température de l'eau en rivière. Can. J. Civ. Eng. 13, 352–364.
Milner, A.M., Brown, L.E., Hannah, D.M., 2009. Hydroecological response of river systems to shrinking glaciers. Hydrol. Process. 23, 62–77.
Mitchell, S., 1999. A simple model for estimating mean monthly stream temperatures after riparian canopy removal. Environ. Manage. 24, 77–83.
Moore, R.D., Sutherland, P., Gomi, T., Dhakal, A., 2005. Thermal regime of a headwater stream within a clearcut, coastal British Columbia, Canada. Hydrol. Process. 19, 2591–2608.
Null, S.E., Deas, M.L., Lund, J.R., 2009. Flow and water temperature simulation for habitat restoration in the Shasta River, California. River Res. Appl. 26, 663–681.
Oke, T.R., 1987. Boundary Layer Climates, second ed. Metheuen, London.
Schiermeier, Q., 2006. On thin ice. Nature 441, 147–148.
Selker, J.S., Thévenaz, L., Huwald, H., Mallet, A., Luxemburg, W., Van de Giesen, N., Stejskal, M., Zeman, J., Westhoff, M., Parlange, M.B., 2006. Distributed fiber optic temperature sensing for hydrologic systems. Water Resour. Res. 42, W12202.
Sinokrot, B.A., Stefan, H.G., 1993. Stream temperature dynamics – measurements and modelling. Water Resour. Res. 29, 2299–2312.
Sridhar, V., Sansone, A.L., Lamarche, J., Dubin, T., Lettenmaier, D.P., 2004. Prediction of stream temperature in forested watersheds. J. Am. Water Res. Assoc. (JAWRA) 40, 197–214.
Story, A., Moore, R.D., Macdonald, J.S., 2003. Stream temperatures in two shaded reaches below cutblocks and logging roads: downstream cooling linked to subsurface hydrology. Can. J. For. Res. 33, 1383–1396.
Tonolla, D., Acuna, Vicenc, Uehlinger, U., Frank, T., Tockner, K., 2010. Thermal Heterogeneity in River Floodplains. Ecosystems 13, 727–740.
Torgersen, C.E., Faux, R.N., McIntosh, B.A., Poage, N.J., Norton, D.J., 2001. Airborne thermal remote sensing for water temperature assessment in rivers and streams. Remote Sens. Environ. 76, 386–398.
Turner, M.G., 1990. Spatial and temporal analysis of landscape patterns. Landscape Ecol. 4, 21–30.
Turner, A.G.D., 2010. Stream Temperature Grid Generalisation Source Code Web Page. <http://www.geog.leeds.ac.uk/people/a.turner/src/andyt/java/projects/StreamTemperatureGridGeneralisation/> (last accessed 10.11.10).
Webb, B.W., Zhang, Y., 1999. Water temperatures and heat budgets in Dorset chalk water courses. Hydrol. Process. 13, 309–321.
Webb, B.W., Hannah, D.M., Moore, R.D., Brown, L.E., Nobilis, F., 2008. Recent advances in stream and river temperature research. Hydrol. Process. 22, 902–918.
Webb, B.W., Zhang, Y., 1997. Spatial and seasonal variability in the components of the river heat budget. Hydrol. Process. 11, 79–101.
Westhoff, M.C., Savenije, H.H.G., Luxemburg, W.M.J., Stelling, G.S., van de Giesen, N.C., Selker, J.S., Pfister, L., Uhlenbrook, S., 2007. A distributed stream temperature model using high resolution temperature observations. Hydrol. Earth Syst. Sci. 11, 1469–1480.
WLDelft, 2011. Delft3D User and Technical Support Manuals. <http://oss.deltares.nl/web/hydrodynamics/rivers> (last accessed 18.08.11).
Young, R.G., Collier, K.J., 2009. Contrasting responses to catchment modification among a range of functional and structural indicators of river ecosystem health. Freshw. Biol. 54, 2155–2170.
Younus, Y., Hondzo, M., Engle, B.A., 2000. Stream temperature dynamics in upland agricultural watersheds. J. Environ. Eng. – ASCE 126, 518–526.

Please cite this article in press as: Carrivick, J.L., et al. Numerical modelling of spatio-temporal thermal heterogeneity in a complex river system. J. Hydrol. (2011), doi:10.1016/j.jhydrol.2011.11.026